

Cryogenic measurement set-up for characterization of superconducting nano structures for single-photon detection applications

Manju Singh¹, Rishu Chaujar² and R. K. Rakshit^{1,*}

¹Academy of Scientific and Innovative Research, CSIR-NPL Campus, Dr K. S. Krishnan Marg, New Delhi 110 012, India and National Physical Laboratory, Council of Scientific and Industrial Research, Dr K. S. Krishnan Marg, New Delhi 110 012, India

²Microelectronics Research Lab, Department of Engineering Physics, Delhi Technological University, Bawana Road, Delhi 110 042, India

We discuss the design and development of a cryogenic set-up down to ~1.8 K for carrying out measurements on superconducting nanowire single-photon detectors. The set-up consists of two separate low-temperature inserts, one for electrical characterization and the other for optical measurements and characterization of single-photon detectors. A sample holder with necessary arrangements for precise alignment of laser light with the active area of the device to enhance optical coupling efficiency has been designed for the optical probe. The invar alloy has been used for the sample holder to ensure that the alignment is not disturbed at low temperature. Single-mode fibres due to their high transmission rate, minimum attenuation and least distortion have been used to shine light on the samples. The sample holder with 20-pin LCC socket and matching chip carrier provides convenient and fast sample mounting in the electrical insert. Mu-metal has been employed to cover the sample space in both the inserts in order to attenuate any electromagnetic interference. Temperature stability with the passage of time has been monitored. It has been found that variation in temperature is less than 10 mK at the lowest operating temperature. Another important advantage of the system is its low enough liquid helium loss rate (~100 ml/h) with all inserts, which allows uninterrupted measurements for several days without any refilling of liquid helium.

Keywords: Device packaging, optical alignment, liquid helium cryostat, low temperature measurement probe.

QUANTUM optical technologies have many applications in the area of quantum teleportation¹⁻³, quantum computation (QC)⁴ and quantum key distribution (QKD)⁵⁻⁹. These applications rely significantly on the performance of single-photon detectors. Photo multiplier tube (PMT) is one of the initially invented photon detectors. Si-based avalanche photo diode (APD) has better performance matrices in comparison to PMT¹⁰. However, both these technologies

have limitation at telecom wavelengths. Although InGaAs-based photo detector shows better detection efficiency at infrared, it has shortcomings due to high dark count rate, relatively large time jitter, low count rate and after-pulsing effect¹¹. Superconducting nanowire single-photon detectors (SNSPDs) have shown potential in recent years for applications in the area of quantum optical technologies due to better performance matrices¹²⁻¹⁹.

It has been found that the detection efficiency of SNSPDs increases and the dark count diminishes significantly with decrease in operating temperature. Motivated by the earlier work of Orgiazzi *et al.*²⁰, on an experimental set-up down to 4.2 K which was based on standard liquid helium transport dewar, we have designed and built a liquid helium flow cryostat down to 1.8 K along with probes for electrical as well as optical characterization. Economical consumption of liquid helium, sound temperature stability, efficient optical coupling, and easy and user-friendly sample changing option without breaking the vacuum or warming up the cryostat were some of the important requirements taken into consideration while designing the cryostat.

The cryogenic set-up

Cryostat

High efficiency variable temperature from 1.8 to 325 K with liquid nitrogen-shielded liquid helium has been custom-designed and manufactured by Cryo Industries of America Inc., Manchester, NH 03103 for use in the characterization of superconducting nanowires and SNSPDs. Figure 1a shows a photograph of the complete set-up. The system has the provision of monitoring cryogen level (both nitrogen and helium). It also has the provision to cool down the sample space below 4.2 K, both in vapour (dynamic exchange gas) and in liquid configuration. The cryostat has four chambers namely, vacuum chamber, liquid nitrogen reservoir, liquid helium reservoir and sample tube space. Figure 1b shows the top view of the

*For correspondence. (e-mail: rakshitrk@nplindia.org)

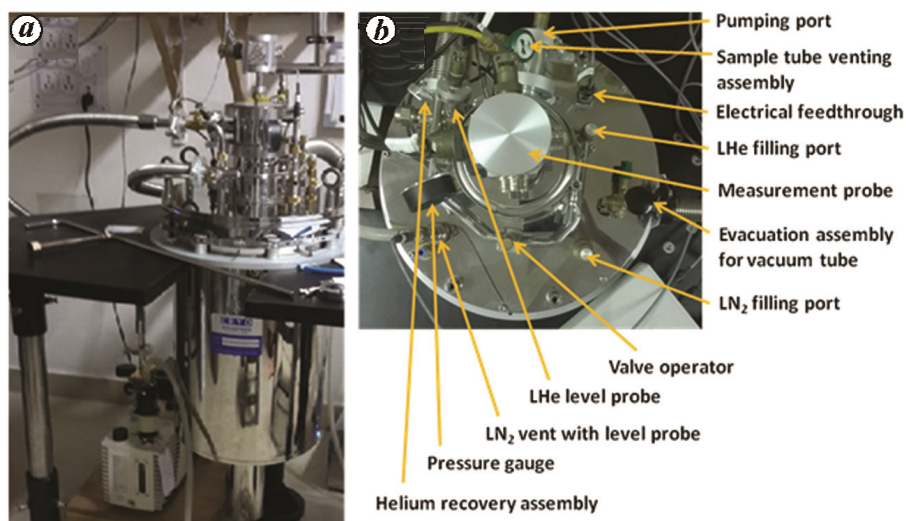


Figure 1. *a*, Photograph of complete cryostat system. *b*, Top view of the system, with major parts marked using arrows.

cryostat. Sample tube venting assembly, pumping port, pressure gauge assembly with safety pressure relief valve are used for regulating and monitoring pressure in the sample tube space. Two-stage rotary vane pumping station along with vacuum gauge, oil mist exhaust filter and pumping line assembly have been used to pump the sample space. The outer vessel called vacuum tube acts as a thermal insulator. The evacuation assembly with safety pressure relief valve attached to the vacuum tube can be connected to a turbo molecular pump. The system is also equipped with an internal charcoal getter. It allows the system to operate with a mechanical roughing pump evacuation.

Helium-filled port is fitted with helium flow control valve, safety pressure relief valve, and at the end it is connected with helium recovery line. Liquid helium flows from the reservoir through the adjustable flow valve down to the vapourizer/heat exchanger located at the bottom of the sample tube and on applying heat, it vaporizes the liquid. The cold helium vapour enters the sample zone through the capillary and cools the sample space to a selected temperature. De-icing heating coil is installed on the capillary for optional heating.

Liquid helium reservoir has a capacity of 10 litre. Liquid nitrogen reservoir which also has a capacity of 10 litre surrounds the inner helium reservoir to provide full nitrogen shield and thereby reduce helium consumption significantly. Less than 100 ml/h helium loss rate with all inserts enables the user to continue experiments at a stretch for 2–3 days without refilling any cryogen. Dual-channel liquid cryogen level monitor with top-loading removable superconducting liquid helium level probe and capacitance liquid nitrogen level probe mounted inside the cryogen reservoirs enables *in situ* monitoring of liquid helium and nitrogen levels respectively. The level-monitoring assembly prompts to refill

the chamber before it gets empty and assists avoiding any temperature variation at sample space due to shortage of coolant. The system can run without any interruption for several weeks by timely refilling of cryogens.

The sample tube with 3.0 inch outer diameter and 8 inch long tail section provides enough space for sample mounting with all necessary electrical wirings and optical fibres, and flexibility for future up-gradation. Radiation shield tube with 3.5 inch outer diameter inside the tail of the cryostat surrounding the sample space has been used for efficient cooling and low thermal loss. A 50 Ω cartridge heater along with a calibrated (1.4–325 K) cernox sensor is installed on the heat exchanger. The temperature of the heat exchanger is controlled by dual action of regulating helium flow manually and auto adjusting the electrical power supplied to the heater. For monitoring and controlling the temperature of the heat exchanger, the heater and sensor are connected to a Lakeshore 336 auto tune temperature controller outside through hermetic 10-pin electrical feedthrough.

Customized variable temperature insert for electrical measurements

Top-loading sample probe assembly with a sliding seal for sample positioning with interface flange has been designed (Figure 2). Enlarged view of the top and bottom parts of the insert is shown in lower panel of the figure. The probe is made from thin-walled stainless steel tube because of its high mechanical strength and excellent thermal insulation. A T-shaped sample holder has been made from oxygen-free high conductivity copper as its low vapour pressure causes less degassing. A 20-pin LCC socket is mounted on copper sample mount. Non-magnetic LCC20 chip carrier compatible with LCC

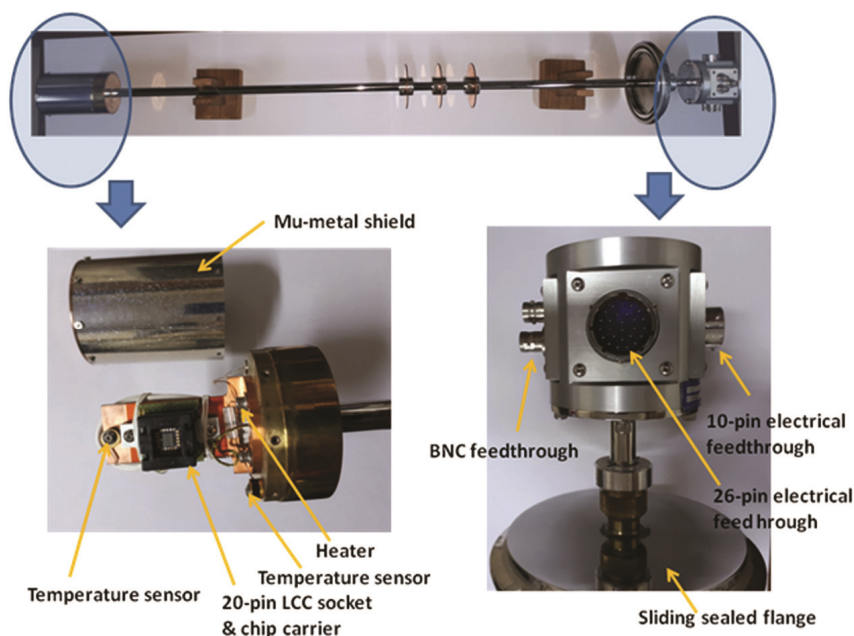


Figure 2. (Top panel) Variable temperature insert for electrical characterization. (Lower panel, left) Major components of the low temperature module. (Lower panel, right) Different feedthroughs for electrical connections.

socket has been employed for sample mounting and necessary electrical wiring for transport measurements. Mu-metal shield is attached to the sample mount to cover the entire sample assembly for shielding against any static or low-frequency magnetic fields.

Hermetic 10-pin electrical feedthrough has been mounted on top of the insert for the temperature sensors and heater. The $50\ \Omega$ cartridge heater and calibrated (1.4–325 K) cernox sensor are installed on brass sample mount with the temperature sensor located inside Mu-metal shield (Figure 2, lower panel – left). Another calibrated (1.4–325 K) cernox sensor has been placed on the copper sample holder next to the LCC socket for accurate measurement of sample temperature. While a 26-pin vacuum-sealed electrical feedthrough has been placed on the probe top for DC transport measurements, six hermetically sealed BNC feedthroughs with coaxial cables have been used for AC transport (Figure 2, lower panel – right). Ten twisted pairs (20 wires) of 36 gauge phosphor bronze wires have been used to connect 20-pin LCC socket to 20 pins of 26-pin feedthrough. Combination of good electrical conductivity and low thermal conductivity of phosphor bronze wires prevent excessive heat load.

Customized variable temperature insert for single-photon detection applications

Similar to the electrical probe, this is a top-loading sample probe assembly with compatible dimensions and seals for height adjustment (Figure 3, top panel). Details of the

sample mount have been shown in the centre panel of Figure 3. It has a brass sample mount with copper end cap and two half cylindrical Mu-metal shield enclosures to cover the entire sample assembly. It carries one $50\ \Omega$ cartridge heater and one calibrated (1.4–325 K) cernox sensor at the T-mount. A miniature calibrated cernox temperature sensor as can be seen in Figure 4 is also mounted on the sample holder body for precise monitoring of sample temperature (Figure 4). A 10-pin vacuum-sealed electrical connector mounted on the body of the outer module (Figure 3, bottom panel) provides access to the temperature controller. The sensor and heater leads running inside a thin-walled stainless steel tube are connected to the inside pins of the 10-pin connectors. Hermetic SMA female-to-female connectors are mounted on the outer module of the insert to provide access to biasing (constant current biasing) the sample, and monitor RF output response from kHz to GHz range due to absorption of photon pulse. One flexible, low-temperature compatible ultra-miniature coaxial cable and one semi-rigid coaxial cable having male SMA connectors at both ends running along the length of the insert. The low-temperature end of these cables is terminated in the sample area inside the Mu-metal shield and can be connected to the sample holder one at a time though a small, semi-rigid coaxial adapter. This adapter is thermally anchored using copper braids with the bottom copper cap and helps in cooling the sample holder. The arrangement provides easy access to sample mounting and optical alignment, and also holds the sample holder firmly inside the cryostat. The probe has provision of shining light onto the sample. Two optical fibres of different wavelengths and

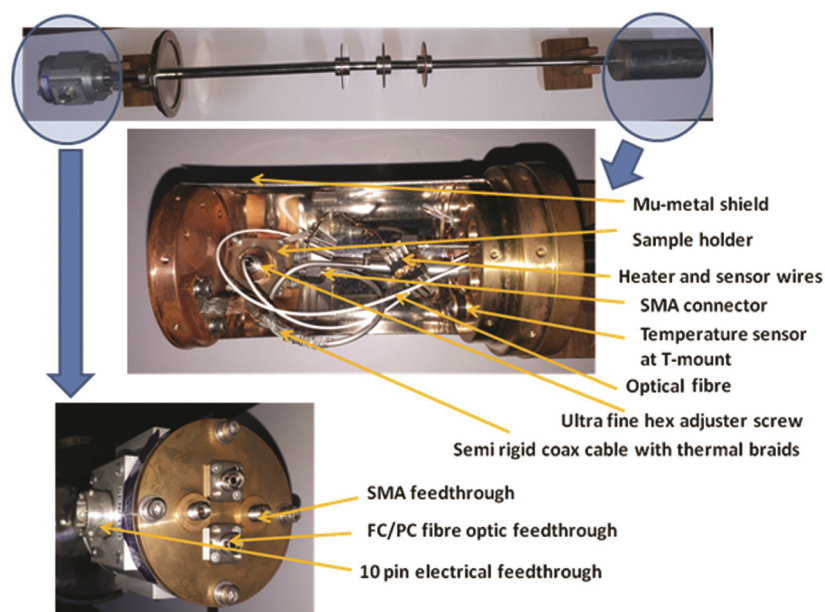


Figure 3. (Top panel) Variable temperature insert for single-photon detection application. (Bottom panel) Enlarged view of top of the insert having feedthroughs for electrical as well as optical connections. (Middle panel) Details of essential components of the optical insert.

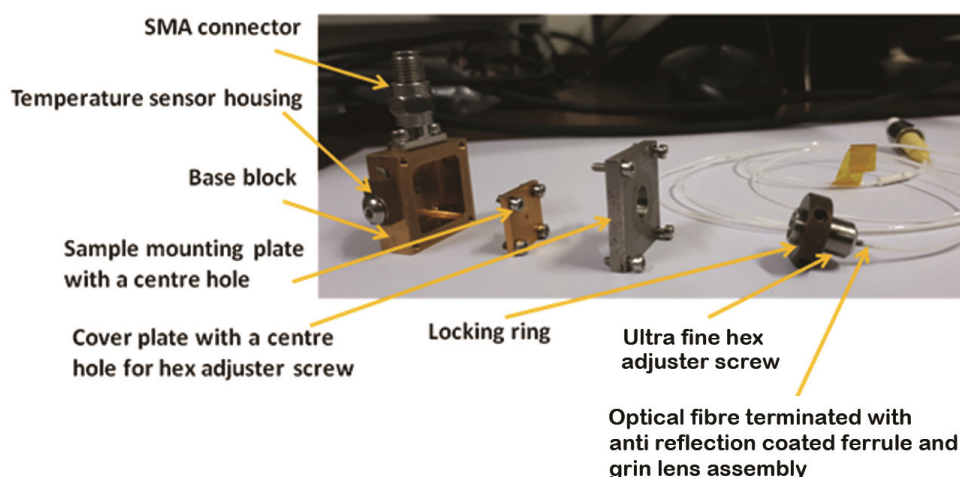


Figure 4. Photograph showing all essential components for a customized sample holder placed in sequence in order to easily understand the sample mounting steps.

about a metre long have been placed inside the stainless steel tube. One end of both the single-mode fibres (SMF-28e or equivalent) while connected to hermetic FC/PC fibre optic feedthrough at the top of the insert other end of them can be fixed on sample holder (one at a time) for illumination of sample.

Customized sample holder for single-photon detection applications

Compatible with the optical insert and available sample space of the cryostat, a customized sample holder has

been designed. It consists of the main body, device-mounting plate and top enclosure (Figure 4), all made out of invar 36 alloy due to its relatively low thermal expansion coefficient compared to other low-temperature compatible materials. The main body and sample mounting plate have thin electroplated gold coating. Single-mode optical fibre with anti-reflection-coated pigtailed ferrule ($\Phi = 1.8$ mm) and graded-index (GRIN) lens assembly has been used to guide laser light onto the active area of the device. An 8° face angle lens has been chosen to minimize back reflection and compensate for the angular beam deviation from angled fibre ferrules. A detailed description can be found elsewhere²⁰.

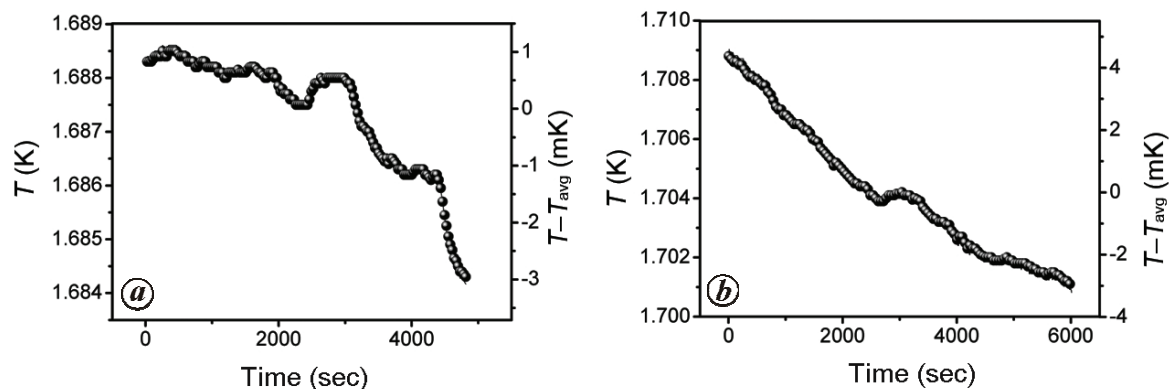


Figure 5. Temperature stability plots. *a*, Plot showing experimental data of temperature drift for electrical insert. *b*, Plot of similar measurements carried out for optical insert.

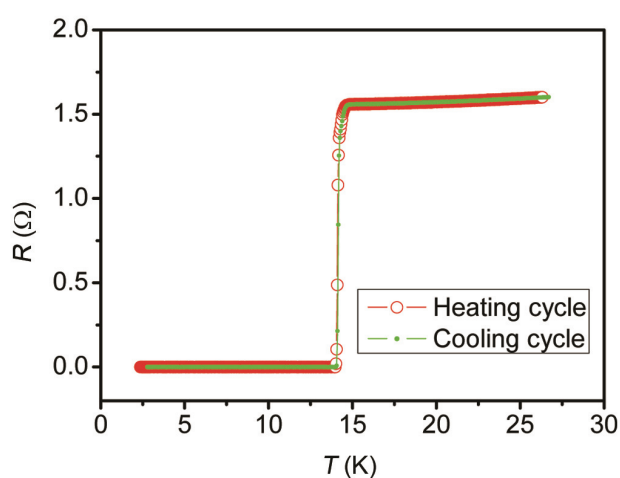


Figure 6. Resistance versus temperature plots of superconducting NbN films. Heating cycle was followed immediately after completion of cooling cycle. The cooling and heating profiles are perfectly superimposed.

As shown in Figure 3, the sensor wires are demountable. The sample holder can be detached by unplugging the low-temperature compatible mini-disconnects during mounting of the sample and alignment under microscope. The process involves: (1) pasting the sample on the sample-mounting plate already fixed firmly inside the main body and placing it as precisely as possible with the help of an ordinary microscope so that the centre of the active area (typically $10\ \mu\text{m} \times 10\ \mu\text{m}$) of the sample coincides with the central hole of the mounting plate; (2) loosely placing the top lid that carries the fibre end onto the main body; (3) placing the whole assembly under a microscope; (4) turning on the laser so that the fibre tip illuminates the sample; (5) fine adjustment of the top lid to ensure that the active area is illuminated, and (6) tightening the screws to firmly fix the top lead onto the main body. For *in situ* monitoring and alignment of laser light,

an assembly consisting of a short-wave infrared camera with InGaAs sensor having spectral band from 0.9 to $1.7\ \mu\text{m}$ (WiDY SWIR 640V-S, New Imaging Technologies, France) along with Optem12.5:1 microscopic zoom lens and focusing module has been developed. Illumination source with the option for both fibre optic-based ring light and coaxial illuminator is integrated with the camera.

System performance

The temperature stability of both the inserts has been checked and plotted (Figure 5). Inserts are cooled down and after stabilization of temperature using the adjustable flow valve, variation of temperature is monitored with time. It is important to mention that during these measurements neither the vapourizer heater nor the sample mount heater is used to stabilize the probe temperature. While the maximum temperature drift of $\sim 4\ \text{mK}$ from the average value has been observed for the electrical insert, the optical insert shows maximum drift of $\sim 7\ \text{mK}$ over a time-span of about $1\frac{1}{2}$ hours.

Figure 6 shows the temperature dependence of resistance change in superconducting NbN thin films carried out in four-point-probe measurement geometry. Measurements in both heating and cooling cycle are performed under dynamic thermal condition at a sweeping rate of $0.5\ \text{K/min}$. The data clearly show superconducting transition (T_c) at $14.6\ \text{K}$ with $0.5\ \text{K}$ transition width (ΔT). The calculated resistance values in the heating and cooling cycle follow each other, showing the absence of any thermal hysteresis associated with the measurement system.

Conclusion

We have designed and developed a cryogenic measurement set-up for single-photon applications in the temperature range $1.8\text{--}325\ \text{K}$. Two dedicated inserts have

been designed. The electrical insert will be used for optimization of superconducting properties in nano structures for their application as single-photon detectors by systematic studies of transport properties below and above T_c . The optical insert has all the provisions for detailed studies of superconducting nano structures for evaluating their ability as single-photon detectors. It also has the provision and space for future up-gradation for mounting and study of two single-photon devices at a time, and some specific studies such as time-correlated single-photon counting.

1. Yin, J. *et al.*, Quantum teleportation and entanglement distribution over 100-kilometre free-space channels. *Nature*, 2012, **488**, 185–188.
2. Xiao-Song Ma, X.-S. *et al.*, Quantum teleportation over 143 kilometres using active feed-forward. *Nature*, 2012, **489**, 269–273.
3. Takesue, H., Dyer, S. D., Stevens, M. J., Verma, V., Mirin, R. P. and Nam, S. W., Quantum teleportation over 100 km of fiber using highly efficient superconducting nanowire single-photon detectors. *Optica*, 2015, **2**, 832–835.
4. Hadfield, R. H., Single-photon detectors for optical quantum information applications. *Nature Photonics*, 2009, **3**, 696–705, and references therein.
5. Wang, S. *et al.*, 2 GHz clock quantum key distribution over 260 km of standard telecom fiber. *Opt. Lett.*, 2012, **37**, 1008–1010.
6. Yao, X.-C. *et al.*, Experimental demonstration of topological error correction. *Nature*, 2012, **482**, 489–494.
7. Shimizu, K. *et al.*, Performance of long-distance quantum key distribution over 90-km optical links installed in a field environment of Tokyo metropolitan area. *J. Lightwave Technol.*, 2014, **32**, 141–151.
8. Northup, T. E. and Blatt, R., Quantum information transfer using photons. *Nature Photonics*, 2014, **8**, 356–363.
9. Korzh, B. *et al.*, Provably secure and practical quantum key distribution over 307 km of optical fibre. *Nature Photonics*, 2014, **9**, 163–168.
10. Yuana, Z. L., Dynes, J. F. and Shields, A. J., Resilience of gated avalanche photodiodes against bright illumination attacks in quantum cryptography. *Appl. Phys. Lett.*, 2011, **98**, 231104(1–3).
11. Itzler, M. A. *et al.*, Advances in InGaAsP-based avalanche diode single photon detectors. *J. Mod. Opt.*, 2011, **58**, 174–200.
12. Gol'tsman, G. N. *et al.*, Picosecond superconducting single-photon optical detector. *Appl. Phys. Lett.*, 2001, **79**, 705–707.
13. Eisaman, M. D., Fan, J., Migdal, A. and Polyakov, S. V., Invited review article: Single-photon sources and detectors. *Rev. Sci. Instrum.*, 2011, **82**, 071101(1–25), and references therein.
14. Natarajan, C. M., Tanner, M. G. and Hadfield, R. H., Superconducting nanowire single-photon detectors: physics and applications. *Supercond. Sci. Technol.*, 2012, **25**, 063001(1–16), and references therein.
15. Lita, A. E., Miller, A. J. and Nam, S. W., Counting near-infrared single-photons with 95% efficiency. *Opt. Express*, 2008, **16**, 3032–3040.
16. Miki, S. *et al.*, Large sensitive-area NbN nanowire superconducting single-photon detectors fabricated on single-crystal MgO substrates. *Appl. Phys. Lett.*, 2008, **92**, 061116(1–3).
17. Korneev, A. *et al.*, Recent nanowire superconducting single-photon detector optimization for practical applications. *IEEE Trans. Appl. Supercond.*, 2013, **23**, 2201204(1–4).
18. Salim, A. J., Eftekharian, A. and Majedi, A. H., High quantum efficiency and low dark count rate in multi-layer superconducting nanowire single-photon detectors. *J. Appl. Phys.*, 2014, **115**, 054514(1–4).
19. Akhlaghi, M. K., Atikian, H., Eftekharian, A., Loncar, M. and Majedi, A. H., Reduced Dark Counts in Optimized Geometries for Superconducting Nanowire Single Photon Detectors. *Opt. Express*, 2012, **20**, 23610–23616.
20. Orgiazzi, J.-L. F.-X. and Majedi, A. H., Robust packaging technique and characterization of fiber-pigtailed superconducting NbN nanowire single photon detectors. *IEEE Trans. Appl. Supercond.*, 2009, **19**, 341–345.

ACKNOWLEDGEMENTS. We thank the Director, CSIR-NPL India for support; Prof. A. Hamed Majedi (University of Waterloo, Canada) for fruitful discussions and Cryo Industries of America Inc. for discussions while designing and manufacturing the set-up. This study is supported by the Council of Scientific and Industrial Research, India under the CSIR XII Five-Year Network Project (PSC-0110).

Received 17 December 2017; revised accepted 11 June 2018

doi: 10.18520/cs/v115/i6/1085-1090